Mg/Ca paleothermometry in high salinity environments

Babette A.A. Hoogakker [a,*], Gary P. Klinkhammer [b], Harry Elderfield [a], Eelco J. Rohling [c], Chris Hayward [a,d]

[a] Department of Earth Sciences, University of Cambridge, Downing Street, CB2 3EQ, Cambridge, UK
[b] Oregon State University, College of Oceanic and Atmospheric Sciences, Ocean. Admin. Bldg. 104, Corvallis, Oregon, 97331, USA
[c] National Oceanography Centre, University of Southampton, SO14 3ZH, Southampton, UK
[d] School of Geosciences, Grant Institute of Earth Sciences, University of Edinburgh, Kings Buildings, West Mains Road, Edinburgh EH9 3JW, UK

ARTICLE INFO

ABSTRACT

Planktonic foraminiferal Mg/Ca ratios have become a fundamental temperature proxy in past climate reconstructions. However, in the highly evaporative seas of the tropics and subtropics, anomalously high planktonic foraminiferal Mg/Ca ratios arise, possibly linked to high salinities. The extent to which salinity affects Mg uptake into foraminiferal calcite remains disputed. Some studies suggest only minor salinity effects, whereas others suggest a dominant role. Here, we present new data from the highly saline (>40) Red Sea, which separate pure foraminiferal calcite from other phases. The results show that high Mg/Ca ratios (7 to 13 mmol/mol), found by conventional analysis of planktonic foraminifera from a Red Sea sediment core, are not caused by increased Mg uptake into foraminiferal calcite in a high salinity setting (e.g. beyond those predicted by culturing studies), but instead result from secondary high Mg-calcite overgrowths. The overgrowths likely formed near the sediment–seawater interface, from $CaCO_3$ supersaturated interstitial seawater.

© 2009 Elsevier B.V. All rights reserved.

1. Introduction

To fully appreciate the complexity of climate change, a thorough knowledge of past ocean hydrography and circulation is required. Heat exchange between the atmosphere and ocean takes place at the sea surface. Variations in this heat exchange play a crucial role in climate change, and it is essential that we develop reliable estimates of sea surface temperatures (SST) and salinity, which together determine ocean density (hence, circulation), as well as global ice volume/sea-level (Curry et al., 2003).

Sea water temperature reconstructions based on Mg/Ca ratios in planktonic foraminiferal calcite in addition offer the potential for reconstructing depth-specific (seasonal) temperature, given that the ecology of the investigated planktonic foraminiferal species is sufficiently constrained. A specific advantage of Mg/Ca for reconstructing sea water temperatures is that it can be paired with $\delta^{18}O_{calcite}$ measurements on the same shells, allowing its use to derive $\delta^{18}O_{water}$ (Elderfield and Ganssen, 2000), which provides critical information about global ice volume and the regional hydrological budget.

Although planktonic foraminiferal Mg/Ca ratios have been widely used as a paleotemperature proxy, it has been found that the conventional approach of this method, that of bulk analysis of foraminifera shells after chemical cleaning, produces anomalously high Mg/Ca ratios in strongly evaporative areas of the tropics and subtropics (e.g. Greater and Little Bahama Bank, Eastern Mediterranean Sea, and Red Sea) (Rosenthal et al., 2000; Lear et al., 2002; Reuning et al., 2005; Ferguson et al., 2008).

Recently, Ferguson et al. (2008) suggested that such anomalously high values occur because salinity may exert an important control on Mg/Ca ratios in planktonic foraminifera, with Mg/Ca ratios being 15–60% higher per salinity unit increase than estimated from published calibrations of Mg/Ca increase with temperature. Such an effect would compromise the applicability of foraminiferal Mg/Ca ratios as a paleo seawater temperature proxy. For example, Caribbean Last Glacial Maximum (LGM) temperatures could be overestimated by more than 2.5 °C (Ferguson et al., 2008). Therefore, it is essential that potential effects of salinity on Mg uptake in

* Corresponding author.
E-mail address: bhoo03@esc.cam.ac.uk (B.A.A. Hoogakker).

foraminifera are constrained. In this study we investigate the cause (s) for anomalously high Mg/Ca ratios (ratios beyond those predicted by culturing studies) measured on downcore sediment samples from the highly saline central Red Sea.

2. Materials and methods

In order to assess direct and indirect effects that salinity may have on planktonic foraminiferal Mg uptake, we measured Mg/Ca ratios using a variety of techniques, on downcore sediment samples from central Red Sea sediment core MD92-1017 (19°23′24″N, 38°40′84″E, 570 m water depth) (Rohling et al., 1998). At present the central Red Sea is characterized by high salinities (38–40), while salinities during glacial sea-level low-stands reached 50 or more (Rohling et al., 1998; Siddall et al., 2003; Boyer et al., 2006), making this an ideal natural location for this purpose.

We used several approaches to measure Mg/Ca ratios on calcite of the planktonic foraminifer *Globigerinoides ruber*, together with high magnification scanning electron microprobe (SEM) imaging: (i) mean batch Mg/Ca ratios on multiple specimens by both conventional methodology and flow-through time resolved analysis, (ii) Mg/Ca ratios of different calcite phases by flow-through time resolved analysis, and (iii) Mg/Ca distribution within the foraminiferal shell by SEM-led electron microprobe analysis (Brown and Elderfield, 1996; Barker et al., 2003; Benway et al., 2003; Anand and Elderfield, 2005) (Fig. 1). *G. ruber* thrives in shallow surface waters (top 50 m) and, as this species does not deposit a calcite crust during gametogenesis, its calcite shell should reflect sea water chemistry of these depths (Caron et al., 1990; Reiss and Hottinger, 1984). The age model of core MD92-1017 is based on oxygen isotope stratigraphy (Hemleben et al., 1996; Rohling et al., 1998; Fenton et al., 2000), which divides $\delta^{18}O$ records in standard glacial and interglacial $\delta^{18}O$ stages (Fig. 1).

2.1. Conventional inductively coupled plasma atomic emission spectroscopy (ICP-AES)

A total of 8 samples were analyzed by ICP-AES. Samples contained between 21 and 26 specimens of *G. ruber* (250–300 μm fraction) with batch weights between 250 and 410 μg. Two intervals were selected, covering interglacial MIS 11.3 and cool substage MIS 11.2 (Fig. 1). Prior

Fig. 1. Oxygen isotope record for core MD92-1017 based on planktonic foraminiferal (*G. ruber*) $\delta^{18}O$ (Rohling et al., 1998), with interglacials periods (uneven Marine Isotope Stages, MIS) being characterized by low $\delta^{18}O$ and glacials (even MIS) by high $\delta^{18}O$, due to preferential sequestration of ^{16}O into continental ice masses (Emiliani, 1955; Shackleton and Opdyke, 1973). Oxygen isotope stages are further subdivided into substages (Imbrie et al., 1984; Prell et al., 1986). Grey triangles indicate intervals where planktonic foraminiferal Mg/Ca ratios were measured using the conventional whole batch ICP-AES approach. Black squares and white circles indicate intervals where Mg/Ca ratios were measured using FT-TRA and SEM-led EMPA.

to cleaning, samples were gently crushed between glass plates to release contaminant material. Samples were cleaned using the technique described by Barker et al. (2003), which includes clay removal through the minimal settling technique in UHQ water and methanol, removal of organic matter through oxidation, optical removal of contaminant coarse grains, and a dilute acid leach to remove adsorbed contaminants from the test fragments. For each interval, a subset of samples was also cleaned using a reductive cleaning step (Yu et al., 2005, after Boyle and Keigwin, 1985). Prior to analysis with ICP-AES, samples were dissolved in 0.075 M HNO_3 and centrifuged in order to settle any remaining small silicate particles. Mg/Ca ratios were measured using a Vista ICP-AES, with 0.29% precision.

2.2. Flow through time resolved analysis (FT-TRA)

A total of 6 samples from MIS 7.2, MIS 11.2 and MIS 11.3 were analyzed using flow-through time resolved analysis (FT-TRA, chromatographic approach to cleaning and dissolving foraminiferal calcite and other types of geological materials, adaptable to a variety of chemical methods; Haley and Klinkhammer, 2002). Samples contained 14 to 15 specimens of *G. ruber* (>250 μm fraction), with batch weights between 209 and 330 μg. A simple chemistry was applied to untreated samples, including a 15 minute rinse with deionized water, followed by dissolution with nitric acid ramped up from 0 to 10 mM over 60 minutes, ending with an additional 5 minute water rinse. FT-TRA results are portrayed as effluent element concentration against run-time (Fig. 2A) and effluent Element–Element concentration (Fig. 2B). Complete separation of the overgrowth and biogenic calcite was not achieved in this study (Fig. 2A2). Mg/Ca ratios of planktonic foraminiferal calcite were estimated from the slope of the linear segment dominated by biogenic calcite in the Element–Element plot (Fig. 2B2).

2.3. Scanning electron microscopy-led electron microprobe analysis (SEM-led EMPA)

Two samples were analyzed by SEM-led EMPA from MIS 6.4 and MIS 9.3 from the 250–300 μm size fraction. Each sample was ultrasonically rinsed with ultra-pure water, dried and then impregnated in epoxy resin under vacuum. Samples were polished to expose foraminiferal test walls in cross section and then carbon coated by vacuum evaporation. SEM images were taken from the foraminiferal cross sections using both secondary and backscatter mode, and used as a mapping tool prior to EMPA. The backscatter mode was used to identify areas of foraminiferal calcite (light appearance on SEM image due to relatively high average atomic number) and impurities (grey appearance on SEM image due to lower average atomic number). A CAMECA SX100 was used for EMPA using 15 kV accelerating voltage and 10 nA beam current with beamsize of 5 μm. Spot measurements were carried out spread across the foraminiferal chambers in order to accommodate for heterogeneity. The following elements were measured: wt.% Ca (detection limit 510 ppm), Mg (detection limit 197 ppm), Fe (detection limit 510 ppm), Si (detection limit 151 ppm), Al (detection limit 46 ppm), Mn (detection limit 235 ppm), Sr (detection limit 209 ppm). The α X-ray lines were used for all elements except Sr, for which the La line was analysed. We used internal laboratory standards diopside (Ca, Si), periclase (Mg), corundum (Al), pure metals (Fe, Mn) and celestine (Sr). Data reduction used the X-Phi method within Cameca's PeakSight software.

2.4. Scanning electron microscope (SEM) images

Inner and outer surfaces of planktonic foraminiferal specimens from MIS 6.4 and 9.3 were photographed using a SEM. Each sample was gently crushed to reveal inner surfaces and then ultrasonically rinsed using ultra-pure water. After drying, samples were mounted on
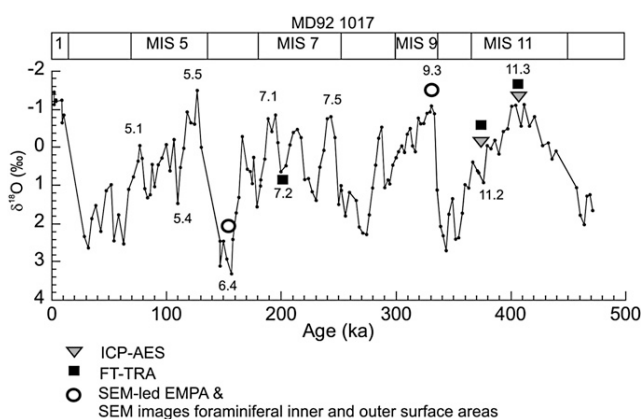
stubs, Au-coated and photographed by a Jeol JSM-820 scanning electron microscope (secondary and backscatter electron images).

3. Results and discussion

Early work by Yusuf (1980) on downcore sediment samples from the Red Sea showed highly elevated planktonic foraminiferal Mg concentrations throughout with the highest values in cold glacial intervals rather than warm interglacials although no cleaning protocol was applied to ensure uncontaminated samples. We find that Mg/Ca ratios obtained using conventional bulk analysis, after a standard Mg/Ca cleaning procedure (Barker et al., 2003), are higher for cold substage MIS 11.2 (10.7–13.0 mmol/mol) than for warm interglacial MIS 11.3 (7.1–7.6 mmol/mol). Using the temperature calibration equation for *G. ruber* (250–300 μm) of Anand et al. (2003), this would give cold substage seawater temperatures of 34–

36 °C, whereas warm interglacial MIS 11.3 would be cooler (30–31 °C). This is at odds with present-day (interglacial) sea water temperatures (27–29 °C; Wyrtki, 1971; Boyer et al., 2006) and a likely reduction of these temperatures by about 4–5 °C during glacial intervals (Siddall et al., 2003; Arz et al., 2007). After the incorporation of a reductive cleaning step, Mg/Ca ratios give calcification temperatures that remain higher for cold substage MIS 11.2 (Mg/Ca 8.4 mmol/mol, 31 °C) than for with warm interglacial MIS 11.3 (Mg/Ca 4.8 mmol/mol, 26 °C) (Table 1).

Results of FT-TRA also reveal the highest whole batch Mg/Ca ratios (19.3–29.3 mmol/mol) for cold substage MIS 11.2 (Table 1). Because no standard Mg/Ca cleaning procedure was applied prior to FT-TRA (without an ultrasonic rinse with ultra-pure water, detrital material like coccoliths and aragonite needles tend to remain fixed to the foraminiferal shell), Mg/Ca ratios are higher than those measured by conventional ICP-AES. The sequential flow-through time resolved
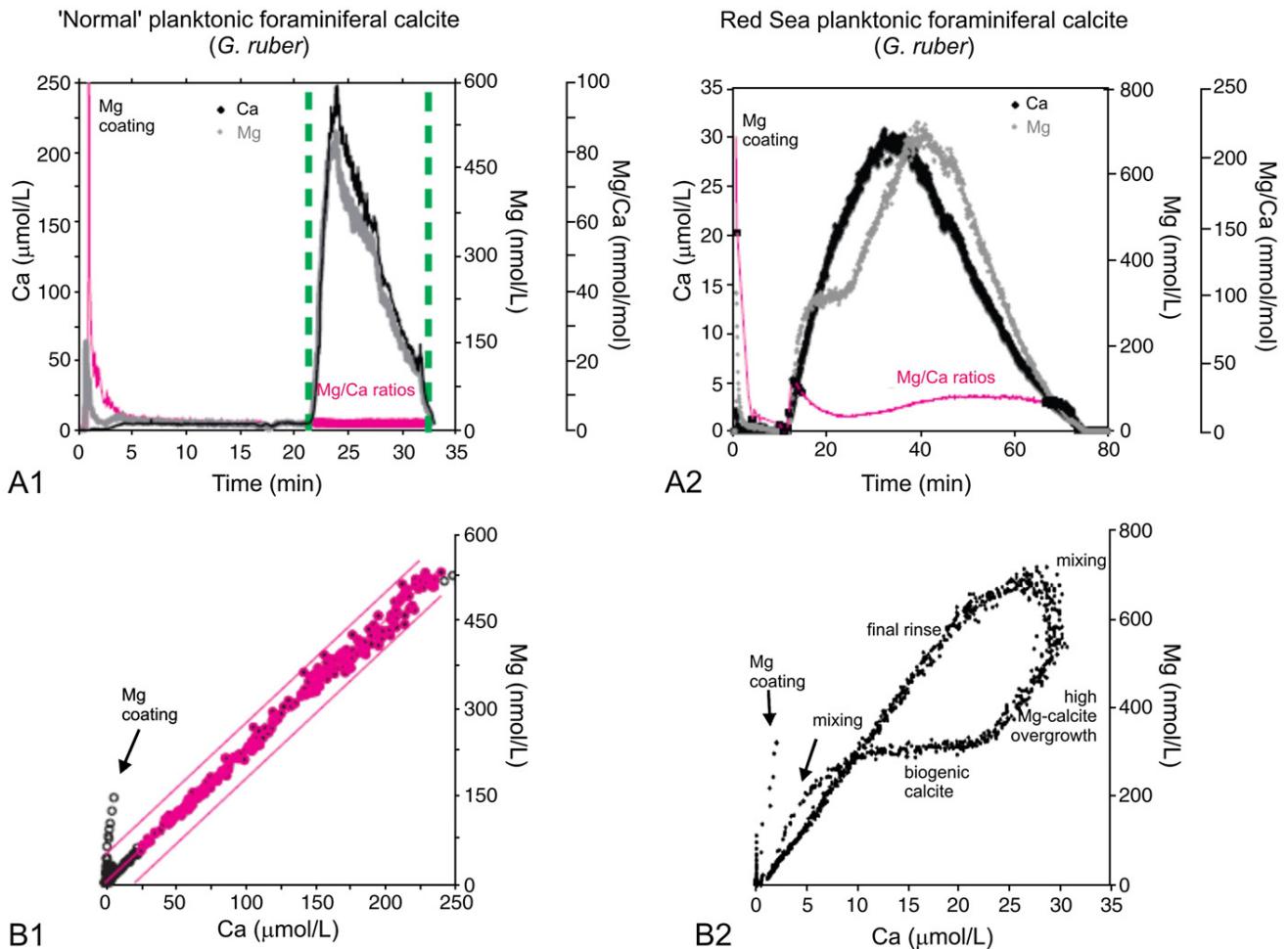

Fig. 2. FT-TRA of specimens of *G. ruber* from a 'normal' salinity setting and from the highly saline Red Sea (MIS 11.2, see Table Table 1). A—Element concentrations (Ca (μmol/L), Mg (nmol/L)) plotted against time for 'normal' *G. ruber* sample from ODP Site 1238 in the North East Equatorial Pacific (A1) and for a *G. ruber* sample from the Red Sea (A2). The typical run-time for a 'normal' sample (A1) is 35 min. Red Sea samples were run for 80 min to attain better phase separation. Samples typically contain Mg coating coming off in the initial rinse with deionized water. Sample A1 was etched with 175 μm HNO₃ for 20 min before dissolution in 10 mM HNO₃ for approximately 10 min. Sample A2 was dissolved in HNO₃ ramped up from 0 to 10 mM over 60 min. In A1 ('normal sample') the Mg peak occurs at the same time as the Ca peak and the peaks have similar shapes. In A2 (Red Sea sample) the Ca peak occurs before the Mg peak and there is a depression in the Mg slope around 20 min. B—Mg and Ca element–element plot for 'normal' *G. ruber* calcite from ODP 1238 (B1) and specimens from the Red Sea (B2). A best-fit line through the biogenic calcite data of A1 (excluding data from the coating) gives a Mg/Ca ratio of 2.25 mmol/mol. Apart from the coating phase, two Mg/Ca phases can be identified in the Red Sea sample (B2): foraminiferal calcite and high Mg-calcite. Biogenic calcite dominates the initial eluate (18–27 min) with relatively low Mg/Ca ratios (A2), causing a depression of the slope in the Element–Element plot. After 27 min dissolved high Mg-calcite dominates the effluent developing a second linear section. The Mg/Ca ratios of the foraminiferal calcite phase can be estimated from the slope of the linear sections that is dominated by the biogenic calcite in the Element–Element plot, assuming that the Ca element concentration curve is controlled by biogenic calcite, giving 2.6 mmol/mol for this sample.

Table 1

A—Details of sea water temperatures and predicted Mg/Ca ratios (using calibration equation of Anand et al. (2003) for *G. ruber* 250–300 μm) for the present day warm interglacials and glacials-cold substages.

	Central Red Sea			
	Present day—warm interglacials		Glacials—cold substages	
	Predicted Mg/Ca ratios 5.3–6.5 mmol/mol	Temperature 50–0 m 27–29 °C	Predicted Mg/Ca ratios 3.2–4.4 mmol/mol	Temperature 50–0 m 22–25 °C

Present day mean annual sea water temperatures for 50–0 m water depths are from Boyer et al. (2006); glacial and cold substage SST from Siddall et al. (2003) and Arz et al. (2007).

B—Measured Mg/Ca ratios, using the various methods discussed in the main text, and their calculated sea water temperatures (same calibration equation as for A).

	Warm interglacials		Glacials—cold substages	
Method	Measured Mg/Ca ratios (mmol/mol)	Calibrated sea water temperatures	Measured Mg/Ca ratios (mmol/mol)	Calibrated sea water temperatures
Conventional ICP-AES, Barker et al. (2003) cleaning protocol	7.6 (MIS 11.3)	31	11.2 (MIS 11.2)	34
	7.1 (MIS 11.3)	30	10.7 (MIS 11.2)	34
	7.2 (MIS 11.3)	30	13.0 (MIS 11.2)	36
Conventional ICP-AES, Barker et al. (2003) cleaning protocol + reductive cleaning step	4.8 (MIS 11.3)	26	8.4 (MIS 11.2)	31
FT-TRA (ICP-MS) whole batch	9.8 (MIS 11.3)	33	19.3 (MIS 7.2)	40
	8.1 (MIS 11.3)	31	24.7 (MIS 11.2)	42
			27.7 (MIS 11.2)	43
			29.3 (MIS 11.2)	44
FT-TRA (ICP-MS) foraminiferal calcite phase	5.2 (MIS 11.3)	27	2.8 (MIS 7.2)	20
	6.3 (MIS 11.3)	29	2.6 (MIS 11.2)	18
			3.2 (MIS 11.2)	22
			3.2 (MIS 11.2)	22
SEM-led EMPA of foraminiferal cross sections (average)	6.4 (MIS 9.3)	29	3.4 (MIS 6.4)	23

C—Predicted Mg/Ca ratios for present-day/warm interglacials and glacials-cold substages, including a salinity effect as proposed by the culturing study of Kısakürek et al. (2008): Mg/Ca = exp((0.06*Salinity + 0.08*Temperature) − 2.8), and a sensitivity to temperature of 0.04 instead of 0.06. Present day mean annual salinity (50–0 m water depth) from Boyer et al. (2006).

	Present day—warm interglacials		Glacials—cold substages	
Predicted Mg/Ca ratios as a function of temperature and salinity (after Kısakürek et al. (2008)	Predicted Mg/Ca ratios	SST, salinity	Predicted Mg/Ca ratios	SST, salinity
	5.4 mmol/mol	27 °C, 38.9	7.1 mmol/mol	22 °C, 50
	6.4 mmol/mol	29 °C, 38.9	9.0 mmol/mol	25 °C, 50
			5.3 mmol/mol	22 °C, 45
			6.7 mmol/mol	25 °C, 45
			3.3 mmol/mol	16 °C, 45
Sensitivity to salinity 0.04	2.5 mmol/mol	27 °C, 38.9	2.6 mmol/mol	22 °C, 50
	2.9 mmol/mol	29 °C, 38.9	3.3 mmol/mol	25 °C, 50

diagram for MIS 11.2 clearly illustrates that the whole-sample ratios are Ca-weighted averages from several Mg-calcite phases: a non-biogenic Mg coating, a high-Mg-calcite phase, and biogenic calcite (Fig. 2). Using

the slope of the linear segment dominated by biogenic calcite (see examples in Fig. 2B) we estimate isolated foraminiferal Mg/Ca ratios of 5.2–6.3 mmol/mol for interglacial MIS 11.3, and 2.8 and 2.6–3.2 for cold
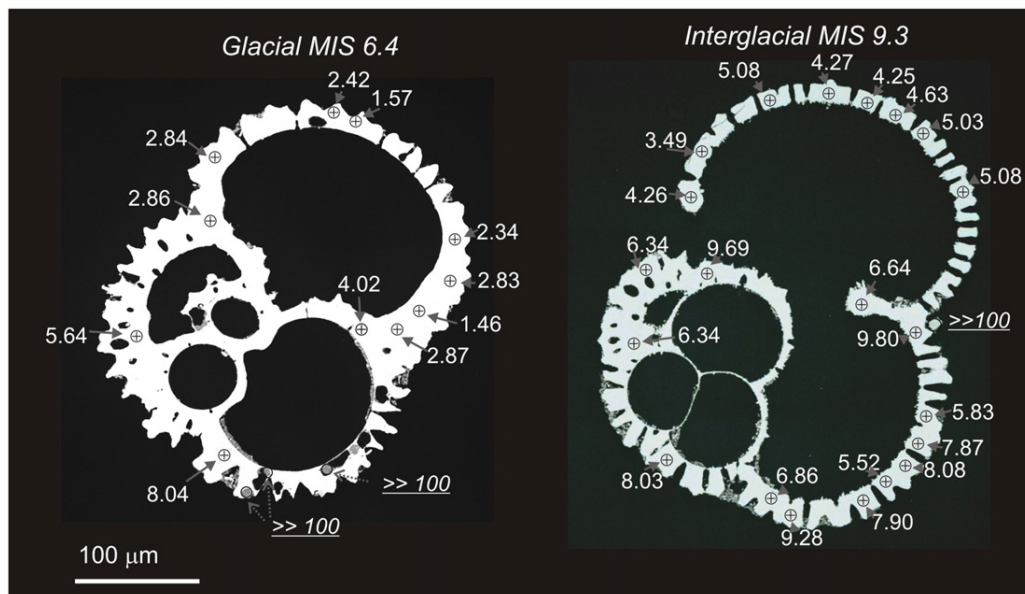

Fig. 3. SEM-led EMPA results with SEM backscattter images of sections across two specimens of *G. ruber* showing the distribution and measured Mg/Ca ratios (mmol/mol) of individual points. The SEM image clearly shows the occurrence of pristine foraminiferal calcite with high reflections in white, and lower reflective areas in grey that have much higher Mg/Ca ratios (underlined italic).

substages MIS 7.2 and 11.2 (Table 1). Using the temperature calibration equation of Anand et al. (2003) for *G. ruber* (250–300 μm) these isolated foraminiferal Mg/Ca ratios give calcification temperatures of 27–29 °C for MIS 11.3 and 20 °C and 18–22 °C for MIS 7.2 and 11.2, which are in good agreement with present-day (interglacial) and cold substage sea water temperatures (Table 1).

SEM-led EMPA for samples from interglacial MIS 9.3 and glacial MIS 6.4 also shows different Mg/Ca phases. High backscatter areas in SEM images of cross sections represent foraminiferal calcite and all have Fe, Si, Al and Mn below detection limit. Low backscatter areas on the other hand represent impure phases that contain significant amounts of Fe, Si, Al and Mn. Foraminiferal Sr/Ca ratios are uniformly distributed (this is confirmed by the FT-TRA analysis) and average 1.65 mmol/mol for both samples, confirming no recrystallization of the tests after burial. The impurities show highly elevated Mg/Ca ratios (≫100 mmol/mol) and comprise a mixture of high-Mg-calcite and silicate minerals (Fig. 3). Average Mg/Ca ratios measured on foraminiferal calcite shell cross sections are 3.4 mmol/mol for glacial MIS 6.4, and 6.4 mmol/mol for interglacial MIS 9.3, giving calcification temperatures of 23 °C for glacial MIS 6 and 29 °C for interglacial MIS 9 (Table 1).

Our results show that planktonic foraminiferal Mg/Ca ratios, obtained from focussed analysis of foraminiferal calcite by FT-TRA and SEM-led EMPA, are in good agreement with present-day (interglacial) sea water temperatures (27–29 °C; Wyrtki, 1971; Boyer et al., 2006) and up to 4–5 °C reduction during glacials and cold substages (Siddall et al., 2003; Arz et al., 2007). Results from both sequential flow-through leaching and SEM-led EMPA show that the higher than predicted Mg/Ca values for interglacials (7.1 mmol/mol) and cold intervals/glacials (13.0 mmol/mol) measured by conventional whole batch ICP-AES are due to impure phases (i.e., not foraminiferal calcite) (Figs. 2 and 3, Table 1). Cleaning techniques used prior to conventional whole batch analysis will remove silicate mineral impurities, and it is therefore most likely that the high Mg/Ca ratios result from other impurities, in particular coatings and overgrowths that are resilient to the applied cleaning procedures. This is further demonstrated by our FT-TRA results, with simultaneous dissolution of the foraminiferal calcite and high Mg-calcite phases throughout the experiment (Fig. 2). Resilience of overgrowths to routinely applied cleaning procedures has also been demonstrated for older Pliocene Caribbean samples (Groeneveld et al., 2008).

Reductive cleaning caused similar reductions in Mg/Ca ratios for both cold MIS 11.2 (33%) and warm interglacial MIS 11.3 (28%) and does not satisfactorily remove the impurities for cold substage MIS 11.2 as Mg/Ca ratios are still higher than those of warm interglacial MIS 11.3 (Table 1). In a recent study, Yu et al. (2007) show that the citrate used in the reductive cleaning step causes preferential leaching of Mg-rich parts of benthic foraminiferal shells. It is not unlikely that the similar reduction in planktonic foraminiferal Mg/Ca ratios of MIS 11.2 and MIS 11.3 after reductive cleaning is due to partial dissolution of Mg-rich parts of the foraminiferal shell rather than removal of impurities (Table 1).

SEM images of the surfaces of slightly crushed and ultrasonically cleaned foraminiferal shells shed further light on the possible origin of the impure phases that cause the high Mg/Ca ratios (Fig. 4). Both samples from interglacial MIS 9.3 and glacial MIS 6.4 show the occurrence of sub-hedral rhombic overgrowths inside and outside foraminiferal chambers, similar to high-Mg-calcite or dolomite rhombs (Fig. 4). Similar overgrowths were observed by Winter (1982) on coccoliths in sediments from the southern Red Sea. Winter (1982) attributed the growth of secondary high Mg-calcite in the Red Sea to interstitial waters being supersaturated with respect to CaCO₃. We propose that the high foraminiferal Mg/Ca ratios measured by conventional whole batch analyses in this study for the Red Sea are due to secondary high-Mg-calcite overgrowths precipitated from CaCO₃ supersatured interstitial sea water (likely near the sediment–sea water
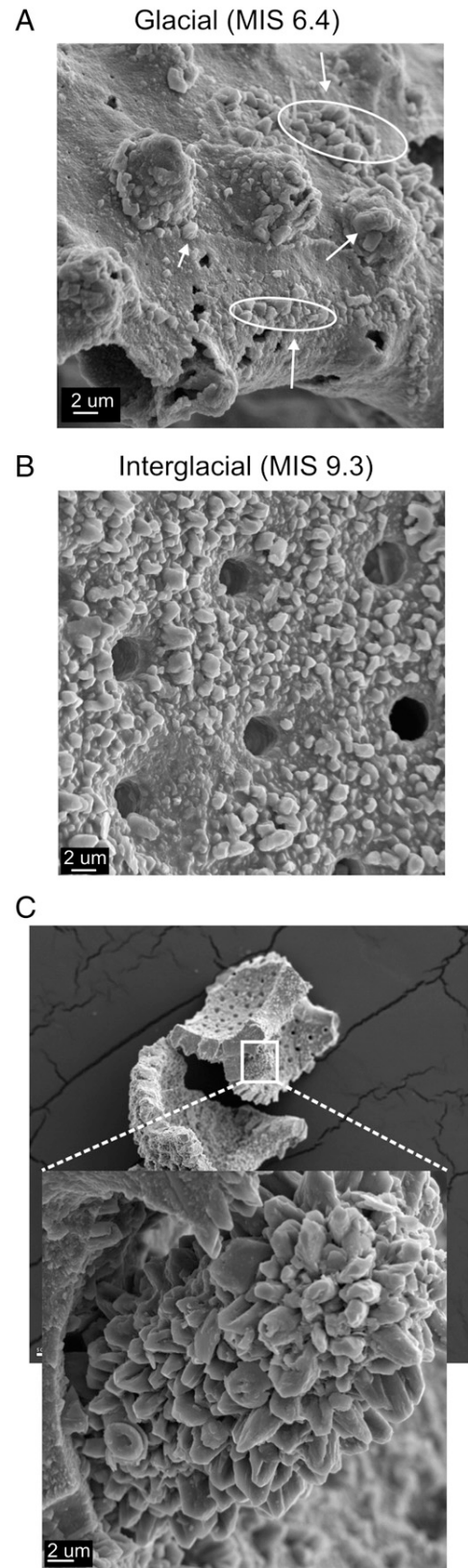

Fig. 4. High resolution SEM photographs of planktonic foraminiferal shell fragments (*G. ruber*) from the central Red Sea from glacial MIS 6.4 (A) and interglacial MIS 9.3 (B, C). Foraminiferal specimens were gently crushed and then ultrasonically cleaned. Subhedral rhombic shaped overgrowths occur outside (A) and inside (B,C) foraminiferal chambers and are suggestive of high-Mg-calcite. Sometimes very large overgrowths can be observed (C).

interface as no increasing downcore trend is observed). A similar mechanism was proposed by Rosenthal et al. (2000) and Lear et al. (2002) to explain higher than expected Mg/Ca ratios in planktonic foraminiferal samples from the Bahamas, confirming that this issue needs to be considered in other areas. Ferguson et al. (2008) argue that high Mg-calcite overgrowths, characterizing foraminiferal samples from the Mediterranean Sea, are generally removed after a reductive cleaning step.

Red Sea high Mg-calcites have $MgCO_3$ contents of ~12–14 mol% (Milliman et al., 1969; Luz et al., 1984). With typical Red Sea overgrowth Mg/Ca ratios of 136 to 163 mmol/mol, we calculate that interglacial samples would need to comprise 3 to 4% overgrowth material, whereas glacial samples would need 2 to 3%, which is within the remit of observations in Fig. 4.

Ferguson et al. (2008) proposed that planktonic foraminiferal Mg/Ca ratios may increase by 15 to 60% per unit increase in salinity. Using these values, planktonic foraminiferal Mg/Ca ratios should have been between 5 and 26 mmol/mol during MIS 6.4 in the central Red Sea, when salinities were 10 or more higher (Rohling et al., 1998; Siddall et al., 2003) yet SEM-led EMPA shows a ratio of only 3.4 mmol/mol (Fig. 3, Table 1). Culture studies suggest a modest increase in planktonic foraminiferal Mg/Ca per unit increase in salinity, varying between 6% (*Orbulina universa, G. ruber*) and 8% (*Globigerinoides sacculifer*) (Nürnberg et al., 1996; Lea et al., 1999; Lea, 2003; Kısakürek et al., 2008). If we predict Mg/Ca ratios with a sensitivity to both temperature and salinity (*G. ruber* calibration equation of Kısakürek et al., 2008), then predicted ratios fall in the range of measured Mg/Ca ratios for interglacials MIS 9.3 and 11.3 (Table 1). For glacial MIS 6.4 predicted Mg/Ca ratios appear too high. If we apply a smaller sensitivity to salinity (4% instead of 6%) measured glacial Mg/Ca ratios do fall within the predicted range (2.6–3.3 mmol/mol), but those predicted for interglacials MIS 9.3 and 11.3 then become to low (2.6–3.1 mmol/mol). This suggests that the sensitivity of planktonic foraminiferal Mg uptake to salinity may be more complex, decreasing with lower temperatures.

Culturing studies suggest that salinity has some effect on Mg uptake in planktonic foraminiferal calcite (Nürnberg et al., 1996; Lea et al., 1999; Kısakürek et al., 2008). Such a mechanism is not responsible for the anomalously high Mg/Ca ratios (7–13 mmol/mol) obtained by conventional analysis for the central Red Sea core we have studied. The results presented do not support a dominant role of salinity on Mg uptake in planktonic foraminiferal calcite in this high salinity environment. Our study emphasizes the key role that carbonate saturation state has on early diagenesis of planktonic foraminiferal calcite through the precipitation of high-Mg-calcite overgrowths. Screening for overgrowths in areas subject to high and/or varying interstitial $CaCO_3$ saturation states, using the methods described in this study, is therefore crucial before interpreting foraminiferal Mg/Ca ratios obtained by conventional methods.

Acknowledgements

References

Anand, P., Elderfield, H., 2005. Variability of Mg/Ca and Sr/Ca between and within the planktonic foraminifers *Globigerina bulloides* and *Globorotalia truncatulinoides*. Geochem. Geophys. Geosys. 6. doi10.1029/2004GC000811.

Anand, P., Elderfield, H., Conte, M.H., 2003. Calibration of Mg/Ca thermometry in planktonic foraminifera from a sediment trap time series. Paleoceanography 18. doi10.1029/2002PA000846.

Arz, H.W., Lamy, F., Ganopolski, A., Nowaczyk, N., Pätzold, J., 2007. Dominant Northern Hemisphere climate control over millennial-scale glacial sea-level variability. Quat. Sci. Rev. 26, 312–321.

Barker, S., Greaves, M., Elderfield, H., 2003. A study of cleaning procedures used for foraminiferal Mg/Ca paleothermometry. Geochem. Geophys. Geosys. 4. doi10.1029/2003GC000559.

Benway, H.M., Haley, B.A., Klinkhammer, G.P., Mix, A.C., 2003. Adaptation of flowthrough leaching procedure for Mg/Ca paleothermometry. Geochem. Geophys. Geosys. 4. doi10.1029/2002GC000312.

Boyer, T.P., Antonov, J.I., Garcia, H.E., Johnson, D.R.R., Locarnini, A., Mishonov, A.V., Pitcher, M.T., Baranova, O.K., Smolyar, I.V., 2006. World ocean database 2005. In: Levitus, S. (Ed.), NOAA Atlas NESDIS 60. U.S. Government Printing Office, Washington, D.C. 190 pp.

Boyle, E.A., Keigwin, L.D., 1985. Comparison of Atlantic and Pacific paleochemical records for the last 215,000 years: changes in deep ocean circulation and chemical inventories. Earth Planet. Sci. Lett. 76, 135–150.

Brown, S.J., Elderfield, H., 1996. Variations in Mg/Ca and Sr/Ca ratios of planktonic foraminifera caused by postdepositional dissolution: evidence of shallow Mgdependent dissolution. Paleocanography 11, 543–551.

Caron, D.A., Anderson, O.R., Lindsey, J.L., Faber, W.W., Lim, E.L., 1990. Effects of gametogenesis on test structure and dissolution of some spinose planktonic foraminifera and implications for test preservation. Mar. Micropaleontol. 16, 93–116.

Curry, R., Dickons, B., Yashayaev, I., 2003. A change in the freshwater balance of the Atlantic Ocean over the past four decades. Nature 426, 826–829.

Elderfield, H., Ganssen, G., 2000. Past temperature and $\delta^{18}O$ of surface ocean waters inferred from foraminiferal Mg/Ca ratios. Nature 405, 442–445.

Emiliani, C., 1955. Pleistocene temperatures. J. Geol. 63, 538–578.

Fenton, M., Geiselhart, S., Rohling, E.J., Hemleben, C., 2000. Aplanktonic zones in the Red Sea. Mar. Micropaleontol. 40, 277–294.

Ferguson, J.E., Henderson, G.M., Kucera, M., Rickaby, R.E.M., 2008. Systematic change of foraminiferal Mg/Ca ratios across a strong salinity gradient. Earth Planet. Sci. Lett. 265, 153–166.

Groeneveld, J., Nürnberg, D., Tiedemann, R., Reichart, G.J., Steph, S., Reuning, L., Crudeli, D., Mason, P., 2008. Foraminiferal Mg/Ca increase in the Caribbean during the Pliocene: Western Atlantic Warm Pool formation, salinity influence, or diagenetic overprint? Geochem. Geophys. Geosys. 9. doi10.1029/2006GC001564.

Haley, B.A., Klinkhammer, G.P., 2002. Development of a flow-through system for cleaning and dissolving foraminiferal tests. Chem. Geol. 185, 51–69.

Hemleben, C., Meischner, D., Zahn, R., AlmogiLabin, A., Erlenkeuser, H., Hiller, B., 1996. Three hundred eighty thousand year long stable isotope and faunal records from the Red Sea: influence of global sea level change on hydrography. Paleoceanography 11, 147–156.

Imbrie, J., Shackleton, N.J., Pisias, N.G., Morley, J.J., Prell, W.L., Martinson, D.G., Hays, J.D., McIntyre, A., Mix, A.C., 1984. The orbital theory of Pleistocene climate: support from a revised chronology of the marine $\delta^{18}O$ record. In: Berger, A., Imbrie, I., Hays, J., Kukla, G., Salzmann, B. (Eds.), Milankovich and Climate: understanding response to astronomical forcing 1. InD. Reidel Publishing Company, Dordrecht, pp. 269–305.

Kısakürek, B., Eisenhauer, A., Böhm, F., Garbe-Schönberg, D., Erez, J., 2008. Controls on shell Mg/Ca and Sr/Ca in cultured planktonic foraminiferan, *Globigerinoides ruber* (white). Earth Planet. Sci. Lett. 273. doi10.1016/j.epsl.2008.06.026.

Lea, D.W., 2003. Elemental and isotopic proxies of marine temperatures. In: The Oceans and Marine Geochemistry (Elderfield, H. ed.) vol. 6 Treatise on Geochemistry (H.D. Holland H.D., K.K. Tuerekian eds.), Elsevier-Pergamon, Oxford, pp. 365–390.

Lea, D.W., Mashiotta, T.A., Spero, H.J., 1999. Controls on magnesium and strontium uptake in planktonic foraminifera determined by live culturing. Geochim. Cosmochim. Acta 63, 2369–2379.

Lear, C.H., Rosenthal, Y., Slowey, N., 2002. Benthic foraminigeral Mg/Ca-paleothermometry: a revised core-top calibration. Geochim. Cosmochim. Acta 66, 3375–3387.

Luz, B., Heller-Kallai, L., Almogi-Labin, A., 1984. Carbonate mineralogy of Late Pleistocene sediments from the Northern Red Sea. Isr. J. Earth-Sci. 33, 157–166.

Milliman, J.D., Ross, D.A., Ku, T.L., 1969. Precipitation and lithification of deep-sea carbonate in the Red Sea. J. Sediment. Petrol. 39, 724–736.

Nürnberg, D., Bijma, J., Hemleben, C., 1996. Assessing the reliability of magnesium in foraminiferal calcite as a proxy for water mass temperatures. Geochim. Cosmochim. Acta 60, 803–814.

Prell, W.L., Imbrie, J., Martinson, D.G., Morley, J.J., Pisias, N.G., Shackleton, N.J., Streeter, H.F., 1986. Graphic correlation of oxygen isotope stratigraphy: application to the late Quaternary. Paleoceanography 1, 137–162.

Reiss, Z., Hottinger, L., 1984. The Gulf of Aqaba, Ecological Micropaleontology. In: Ecological studies, vol. 50. Springer, Berlin, p. 354.

Reuning, L., Reijmer, J.J.G., Betzler, C., Swart, P., Bauch, T., 2005. The use of palaeoceanographic proxies in carbonate periplatform settings—opportunities and pitfalls. Sediment. Geol. 175, 131–152.

Rohling, E.J., Fenton, M., Jorissen, F.J., Bertrand, P., Ganssen, G., Caulet, J.P., 1998. Magnitudes of sea-level lowstands of the past 500,000 years. Nature 394, 162–165.

Rosenthal, Y., Lohmann, G.P., Lohmann, K.C., Sherrell, R.M., 2000. Incorporation and preservation of Mg in Globigerinoides sacculifer: implications for reconstructing the temperature and O-18/O-16 of seawater. Paleoceanography 15, 135–145.

Shackleton, N.J., Opdyke, N.D., 1973. Oxygen isotope and paleomagnetic stratigraphy of Equatorial Pacific Core V28-238: oxygen isotope temperatures and ice volumes on a 10^5 year and 10^6 year scale. Quat. Res. 3, 39–55.

Siddall, M., Rohling, E.J., Almogi-Labin, A., Hemleben, C., Meischner, D., Schmeltzer, I., Smeed, D.A., 2003. Sea-level fluctuations during the last glacial cycle. Nature 423, 853–858.

Winter, A., 1982. Post-depositional shape modification in Red Sea coccoliths. Micropaleontology 28, 319–323.

Wyrtki, K., 1971. Oceanographic Atlas of the International Indian Ocean Expedition. National Science Foundation, Washington DC. 531 pp.

Yu, J., Day, J., Greaves, M., Elderfield, H., 2005. Determination of multiple element/calcium ratios in foraminiferal calcite by quadrupole ICP-MS. Geochem. Geophys. Geosys. 6. doi10.1029/2005GC000964.

Yu, J.M., Elderfield, H., Greaves, M., Day, J., 2007. Preferential dissolution of benthic foraminiferal calcite during laboratory reductive cleaning. Geochem. Geophys. Geosys. 8. doi10.1029/2006GC001571.

Yusuf, N., 1980. Magnesium und Strontium in Foraminiferen-Schalen als Anzeiger für Paleosalinitat. Neues Jahrb. Geol. Paleontol. Mitt. 6, 373–384.